scientific reports

Check for updates

OPEN

Development and in vitro characterization of humanized antibodies for blocking human TRPM4 channel

Shunhui Wei[1,8], Charlene Priscilla Poore[1,8], Ravi Kumar Verma[2], See Wee Low[1,7], Bo Chen[1], Hao Fan[2,3,4]✉ & Ping Liao[1,5,6]✉

Transient receptor potential melastatin 4 (TRPM4) channel, a monovalent cation channel, plays a crucial role in various neurological disorders. We previously showed that TRPM4 activity can be blocked by our antibodies: M4P, which targets rat TRPM4 and M4M, against a similar antigenic epitope of human TRPM4. M4P and M4M demonstrated efficacy in mitigating stroke reperfusion injury. To facilitate human application, M4M was humanized through CDR grafting, resulting in human IgG1 antibodies (Ab1-6). These antibodies were evaluated for their binding affinity, surface staining, stability, and functional inhibition of the human TRPM4 channel. Ab6 (renamed as M4H) was selected and inhibited TRPM4 currents in human brain microvascular endothelial cells under ATP depletion conditions. Importantly, Ab6 (M4H) suppressed ATP depletion-induced cell swelling, indicating its potential for managing vascular injury in ischemic brain diseases. Future studies on animal models could advance the development of novel therapies of neurological disorders with vascular injury.

Keywords TRPM4 channel, Antigenic epitope, Humanized antibody, Channel blocking, Neurological disorder therapy

Transient receptor potential cation channel subfamily M member 4 (TRPM4) is a nonselective monovalent cation channel[1]. Being a unique transient receptor potential channel, it is not permeable to Ca^{2+} but can be activated by an increased intracellular Ca^{2+} level. The presence of ATP helps inhibit TRPM4, and enhanced TRPM4 activity is often observed when there is a decrease in ATP levels[2–5]. Elevated intracellular Ca^{2+} and lower ATP concentration are common features following cerebral hypoxia/ischemia[6–8]. Furthermore, TRPM4 expression is induced in various cell types in many neurological disorders, resulting in a substantial increase in channel activity[5,9,10]. Excessive Na^{2+} influx via TRPM4 causes oncotic cell death[11] and is associated with neuronal excitotoxicity[12].

As current TRPM4 blockers either lack specificity or act on TRPM4 interacting subunits[13]. For example, 9-phenanthrol is widely used in the laboratory to block TRPM4. However, it also inhibits TMEM16A channel in blood vessels[14]. As a member of polycyclic aromatic hydrocarbons, potential toxicity could be linked to cancer, cardiovascular diseases and poor development[15]. Another widely studied TRPM4 blocker is glibenclamide[16]. Glibenclamide blocks TRPM4 via associated unit SUR1. SUR1 is an important subunit of K_{ATP} channel which is crucial for regulating insulin secretion. Thus, glibenclamide is used in clinical practice to manage diabetes[17]. In view of the problems with current TRPM4 blockers, we have developed a polyclonal antibody M4P against rodent TRPM4[21]. M4P binds to an extracellular domain of TRPM4 that is close to the channel pore. Binding of M4P not only directly blocks TRPM4 currents, but also downregulates surface expression of TRPM4 after prolonged incubation. M4P demonstrates therapeutic potential by reducing reperfusion injury in animal

[1]Calcium Signalling Laboratory, Department of Research, National Neuroscience Institute, Singapore 308433, Singapore. [2]Bioinformatics Institute (BII), Agency for Science Technology and Research (A*STAR), Singapore 138671, Singapore. [3]Synthetic Biology Translational Research Program, Yong Loo Lin School of Medicine, National University of Singapore, Singapore 117597, Singapore. [4]Department of Biochemistry, Yong Loo Lin School of Medicine, National University of Singapore, Singapore 117596, Singapore. [5]Duke-NUS Medical School, Singapore 169857, Singapore. [6]Health and Social Sciences, Singapore Institute of Technology, Singapore 138683, Singapore. [7]Present address: National Dental Centre Singapore, Singapore 168938, Singapore. [8]These authors contributed equally: Shunhui Wei and Charlene Priscilla Poore. ✉email: fanh@bii.a-star.edu.sg; ping_liao@nni.com.sg

models of ischemic stroke. Importantly, the vascular protective effects of M4P were retained in a delayed stroke reperfusion model, suggesting the potential to extend the currently narrow reperfusion time window[18].

M4P is a polyclonal antibody raised against rat TRPM4, whereas M4M is a mouse monoclonal antibody targeting a similar antigenic epitope close to the human TRPM4 channel pore[10]. M4M is specific for human TRPM4 and does not cross-react with rodent TRPM4. A transgenic rat model was generated, which carries part of the human TRPM4 sequence that can be recognized by M4M. The therapeutic potential of M4M was demonstrated in vivo by its ability to alleviate reperfusion injury in a rat model of middle cerebral artery occlusion[19]. To study the application of TRPM4 specific antibody in patients in the future, we used the human TRPM4 amino acid sequence of M4M to generate and characterize a series of humanized antibodies, paving the way for therapeutic use of novel TRPM4-blocking antibodies.

Materials and methods

Antibody humanization

A KLH conjugated 21-amino acid antigenic polypeptide (RDSDSNCSSEPGFWAHPPGAQ) which is close to the channel pore of human TRPM4 was used for antibody production. Based on ELISA results, mouse monoclonal antibody (subclass IgG1) M4M demonstrated strong binding affinity and was selected for our study[20]. Antibody humanization was carried out by Genscript Biotech (GenScript) based on the mouse monoclonal antibody M4M. To identify the amino acid sequence of M4M, the antibody was first processed with reduction and alkylation to break the disulfide bonds. The antibody was then digested by six different enzymes: Pepsin, Nonspecific, Trypsin, Chymotrypsin, Asp N, and Lys C. Digestions were analyzed by LC-MS/MS using a Thermo-Fisher Orbitrap Fusion™ mass spectrometer. *De novo* peptide sequencing was performed and assembled into antibody sequences. The structure of parental antibody was carried out by a computer-aided homology modelling program of parental antibody Fv fragments. Sequences were searched against IgBLAST database (NCBI) for identifying the best templates for Fv fragments and especially for building the domain interface. The human acceptor for VH/VL which shared the highest identities to the parental counterparts was selected. Humanized antibodies were designed using CDR grafting.

Briefly, the CDRs of parental antibody were grafted into the human to obtain humanized light chains and humanized heavy chains of IgG1 for each parental antibody. The sequences of the grafted antibody and the parental antibody were compared in the proximity of CDRs, canonical residues, loop interaction, foundation core. Residues that were different in the grafted and parental antibody sequences (i.e. putative back mutation sites) were identified and stepwise incorporation of one or more back mutations were designed in the grafted antibody sequence. The sequence alignment for the 4 heavy chains (VH1, VH2, VH3 and VH4) and 4 light chains (VL1, VL2, VL3 and VL4) are shown in Supplementary Table 1. The heavy and light chains were paired with each other for an affinity ranking experiment. The DNA sequences encoding the chimeric and humanized antibodies heavy and light chains were synthesized and inserted into pcDNA3.4 vector to construct expression plasmids of full-length IgGs.

Plasmid transfection and antibody purification

Expi293F cells (#A14527, Thermo Fisher Scientific) were grown in serum-free Expression Medium for 24 h at 37℃ with atmospheric air containing 8% CO_2 on a shaker. The cells were then transfected with antibody's heavy chain and light chain expression plasmids. For transfection, the reagent was first added into Opti-MEM (#31985070, Thermo Fisher Scientific) and incubated at room temperature for 5 min. The heavy chain expression plasmid and light chain expression plasmid were added to Opti-MEM and then mixed with the transfection medium. After incubation for 20 min, the medium containing the plasmids was added to the Expi293F cells. The cells were cultured at 37℃ and 5% CO_2 for 3 days. The medium and cells were collected and centrifuged at 3000 rpm for 10 min, and the supernatant was collected for antibody purification.

AmMagTM Protein A Magnetic Beads (#vL00695, Genscript) was used to purify the antibody according to the manufacturer's instructions with slight modifications. The tubes containing the Protein A Magnetic Beads slurry were placed on the magnetic separation rack for washing and antibody collection. After washing beads 3 times with PBS and 0.1 M NaOH, the sample containing the antibody was added to the beads and incubated at room temperature for 2 h. The magnetic separation rack was then used to collect the beads and the supernatant was discarded. After washing with 10 column volume of PBS, the antibody eluted from the magnetic beads using 0.05 M Citrate, pH3.5. The eluted antibody was neutralized by adding 1/10 volume of neutralizing buffer (1 M Tris, pH8.5). For further purification, the antibodies were first dialyzed against PBS at room temperature for 2 h. After changing the buffer, the dialysis was repeated for 16 h at 4 °C. Then the antibody was filtered with 0.22 µm membrane filter. The antibody concentration was quantified using the Nanodrop 2000 (Thermo Fisher Scientific) with an extinction coefficient of 1.43.

Western blot

HEK 293 cells grown in 6-well petri dishes were transfected with 4 µg human or mouse TRPM4 plasmid using lipofectamine 2000 transfection reagent (#11668019, Thermo Fisher Scientific). 24 h after transfection, 80 µg of total protein was resolved on 10% SDS-PAGE gels at 80 V, and electrophoretically transferred to PVDF membranes (#1620177, Bio-Rad) at 100 V for 2 h at 4 °C. After blocking with StartingBlock (PBS) blocking buffer (#37538, Thermo Fisher Scientific) for 1 h at room temperature, the membranes were incubated overnight at 4 °C with primary antibodies: Ab1-7 (1:300), M4M (1:300), M4P (1:300) and anti-actin (#A1978, Sigma-Aldrich, 1:1000). After washing away primary antibodies, the membranes were incubated with secondary antibodies against mouse or rabbit IgG for 1 h at room temperature. Primary and secondary antibodies were prepared in StartingBlock (PBS) blocking buffer with 0.05% Tween20 (#P7949, Sigma-Aldrich). Washing buffers contained 0.1% Tween20 dissolved in phosphate-buffered saline (PBS). Amersham ECL Western Blotting Analysis System

(#RPN2109, GE Healthcare) was used and the bands were visualized using a medical X-ray processor (MXP-2000, Kodak). Quantification was done using ImageJ.

Antibody affinity study

For affinity ranking, antibodies were captured on the sensor chip through Fc capture method. Human IgG serves as negative control (NC). Peptide-biotin (RDSDSNCSSEPGFWAHPPGAQ{Lys(biotin)}) was used as the analyte. The surface was regenerated before the injection of another antibody. The process was repeated until all antibodies were analyzed using a Surface Plasmon Resonance (SPR) biosensor, Biacore 8 K (GE Healthcare). The off-rates of antibodies were obtained from fitting the experimental data locally to 1:1 interaction model using the Biacore 8 K evaluation software. The equilibrium dissociation constants (KD) were calculated from the ratio of kd over ka. The antibodies were ranked by their dissociation rate constants (off-rates, kd). Based on the ranking result, the top 3 clones were selected. From these top 3 clones, the affinity measurement of the purified antibody binding to peptide-biotin was individually determined using the Biacore 8 K.

Surface labelling and immunocytochemistry

HEK 293 cells were transfected with myc-tagged human TRPM4 (#RC216888, OriGene Technologies, Inc.) using lipofectamine 2000 transfection reagent (#11668019, Thermo Fisher Scientific). One day after transfection, the cells were incubated with IgG, M4P and M4M at a concentration of 3 μg/ml, and Ab1, 2, 4, and Ab6 (M4H) at a concentration of 0.5 μg/ml for 1 h. After washing with PBS and fixation with 4% paraformaldehyde, the cells were incubated with Wheat Germ Agglutinin (WGA) Alexa Fluor 488 (#W11261, Thermo Fisher Scientific, 5 μg/mL) for 10 min to stain cell membrane. The cells were then permeabilized with 0.1% Triton-X 100 in PBS for 15 min. After blocking with 5% fetal bovine serum for 1 h, the cells were incubated with primary antibody against myc (anti rabbit, #C3956; anti mouse, #M4439. Sigma-Aldrich, 5 μg/mL) for 1 h. After washing away primary antibodies, the cells were incubated with secondary antibodies for 1 h. Secondary antibodies conjugated with Alexa Fluor 647 (anti-mouse or rabbit) and Alexa Fluor 594 (anti-mouse, rabbit, or human) were purchased from Thermo Fisher Scientific. DAPI (#D9542, Sigma-Aldrich, 1 μg/mL) was used to stain nuclei. Fluorescent images were captured with a laser scanning confocal microscope system (FV3000 with software FV31S-SW, Olympus).

Antibody stability assessment

The dynamic light scattering (DLS) system was used to assess antibody aggregation under different temperatures. The aggregate size was quantified using the automated DynaPro® Plate Reader III from Wyatt Technology (Waters Corporation). Using the DYNAMICS software, the Tonset/agg (onset temperature at which aggregates are first detected) was studied to measure the particle size and distribution. The temperature and pH stability of the humanized antibodies were measured using size exclusion-high-performance liquid chromatography (SEC-HPLC) and non-reducing capillary electrophoresis sodium dodecyl sulfate (CE-SDS NR). The temperature stability at 40ºC was tested at various time-points of 0, 7, 14 and 28 days while low pH3.5 stability was measured at 0, 2 and 4 h. In SEC-HPLC test, the 1260 Infinity II Preparative LC System (Agilent Technologies, Inc) was used to measure the percentage of high molecular weight and low molecular weight after exposing to high temperature or low pH. In CE-SDS NR, automated P/ACE MDQ Plus system from Sciex (Sciex) was used to evaluate the main peak of the antibodies. A 10 kDa marker was included as control.

Electrophysiology

The electrophysiological properties of the TRPM4 blocking antibodies were characterized by the whole-cell patch clamp. In brief, HEK293 cells were transfected with 2 μg human TRPM4 (myc-DDK-tagged) using lipofectamine™ 2000 transfection reagent. One day after transfection, whole-cell currents were recorded at room temperature using a patch clamp amplifier (Multiclamp 700B equipped with Digidata 1440 A, Molecular Devices). Patch electrodes were pulled using a Flaming/Brown micropipette puller (P-1000, Sutter Instrument) and polished with a microforge (MF200, WPI Inc). The bath solution contained (in millimole/litre) NaCl 140, $CaCl_2$ 2, KCl 2, $MgCl_2$ 1, glucose 20, and HEPES 20 at pH 7.4. The internal solution contained (in millimole/litre) CsCl 156, $MgCl_2$ 1, EGTA 10, and HEPES 10 at pH 7.2 adjusted with CsOH. WEBMAXC v2.10 was used to calculate the additional Ca^{2+} that was applied to the pipette solution to get 7.4 μM free Ca^{2+}. TRPM4 blocking antibodies or control human IgG were added into bath solution 30 min before recording at a concentration of 0.1–20 μg/ml. From a holding potential of 0 mV, the current–voltage relations were obtained by applying voltage ramps from − 100 to 100 mV for 250 ms. The sampling rate was 20 kHz and filtered at 1 kHz. Current and membrane capacitance data were recorded and analyzed using pClamp10, version10.2 (Molecular Devices). ATP depletion was achieved by applying the oxygen-glucose deprivation (OGD) buffer (bath solution containing 5 mM NaN_3 and replace glucose with 10 mM 2-deoxyglucose (2-DG)) continuously through a MicroFil (34 Gauge, World Precision Instruments Inc) around 10 μm away from the recording cells. The flow rate was set at 200 μL/min. Baseline currents at 0 min were recorded and compared with hypoxic currents recorded 7 min after ATP depletion. Inhibition ratios for different doses of antibodies were calculated by comparing the peak currents at + 80 mV before and after ATP depletion and normalized to IgG for 100%. The IC_{50} values were calculated from the dose-response curves fitted with Sigmoidal dose-response equation with variable slope.

Statistical analysis

Data are expressed as the mean ± SEM Statistical analyses were performed using GraphPad Prism version 6.0. Two-tailed unpaired Student's t test was used to compare two means. Two-way ANOVA with Bonferroni's multiple comparison test was used to analyze time dependent membrane capacitance change.

Results

Production of humanized antibodies against human TRPM4 channel

We have produced a mouse monoclonal antibody M4M against human TRPM4 channel previously[10]. For antibody humanization, M4M was first sequenced to obtain the amino acid sequences of the heavy chain and light chain. Once the sequence was obtained, the complementarity-determining regions (CDRs) for binding to antigen were grafted into the human acceptors to obtain the chimeric antibody Ab1 containing humanized light chain and heavy chain. Subsequent humanized antibodies (Ab2-Ab7) were generated by creating various back mutations of the human antibody origin to the framework (FR) regions of Ab1.

Western blot was first performed to characterize Ab1-Ab7. HEK 293 cells were transfected with human or mouse TRPM4 channels. Polyclonal antibody M4P for rodent TRPM4 serves as a control for recognizing mouse TRPM4[18]. As shown in Fig. 1A, Ab1-7 as well as M4M only bind to human TRPM4 and do not cross-react with mouse TRPM4, whereas M4P is specific for mouse TRPM4. This result is consistent with our

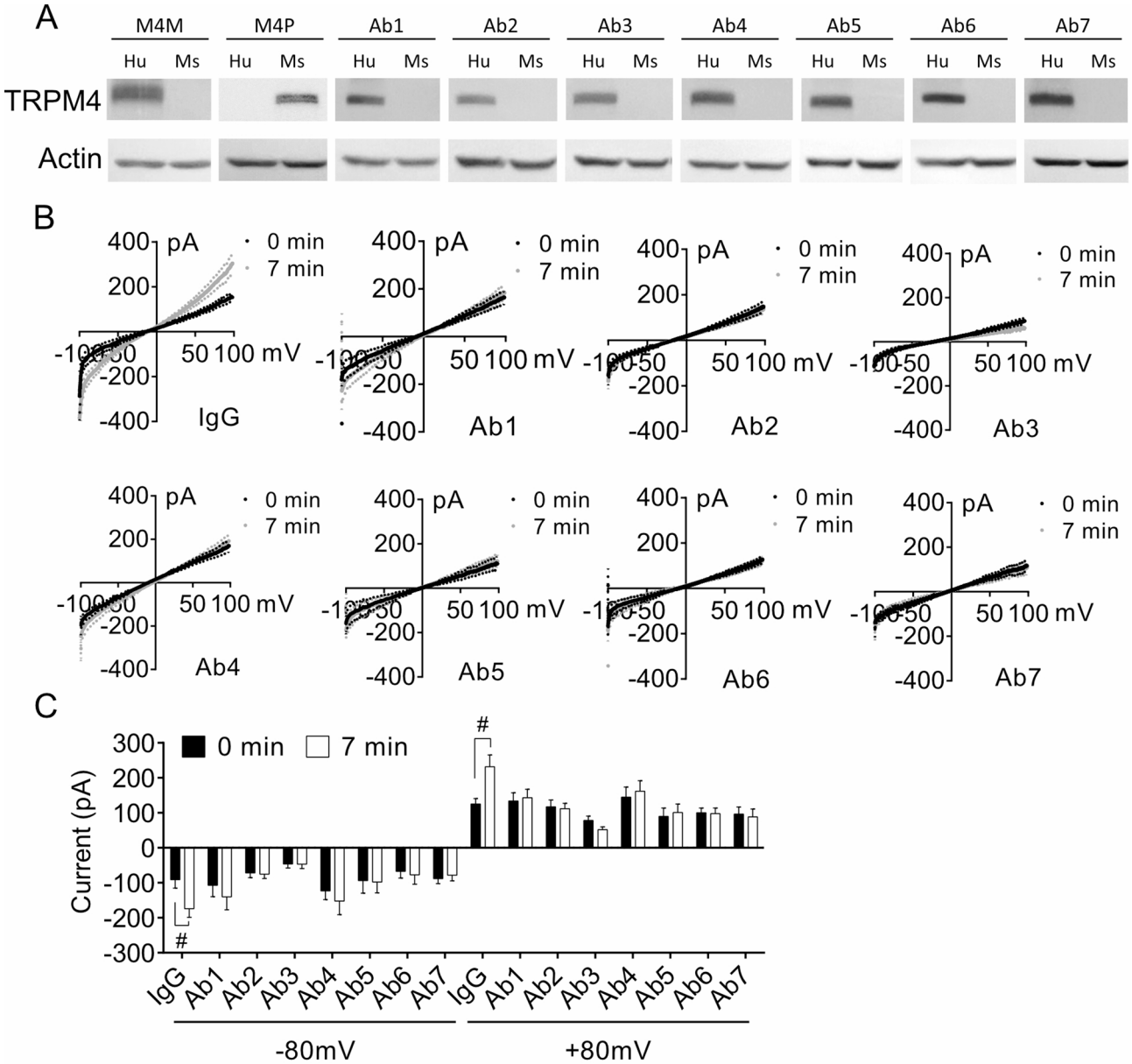

Fig. 1. Characterization of the TRPM4 humanized antibodies. (**A**) HEK 293 cells were transfected with human TRPM4 (Hu) and mouse TRPM4 (Ms). Western blot was performed using the humanized antibodies Ab1-7. M4P was used as negative control and M4M as positive control. (**B**) HEK 293 cells transfected with human TRPM4 were incubated with control human IgG or Ab1-7 at a concentration of 20 μg/ml for 30 min before voltage ramps from − 100 to 100 mV were applied. The current voltage relationships of TRPM4 currents at 0 min baseline and after 7-min ATP depletion were recorded. $N = 6$. (**C**) Comparison of currents before and after 7-min ATP depletion at – 80 mV or 80 mV. # $P < 0.0001$, Student's t test.

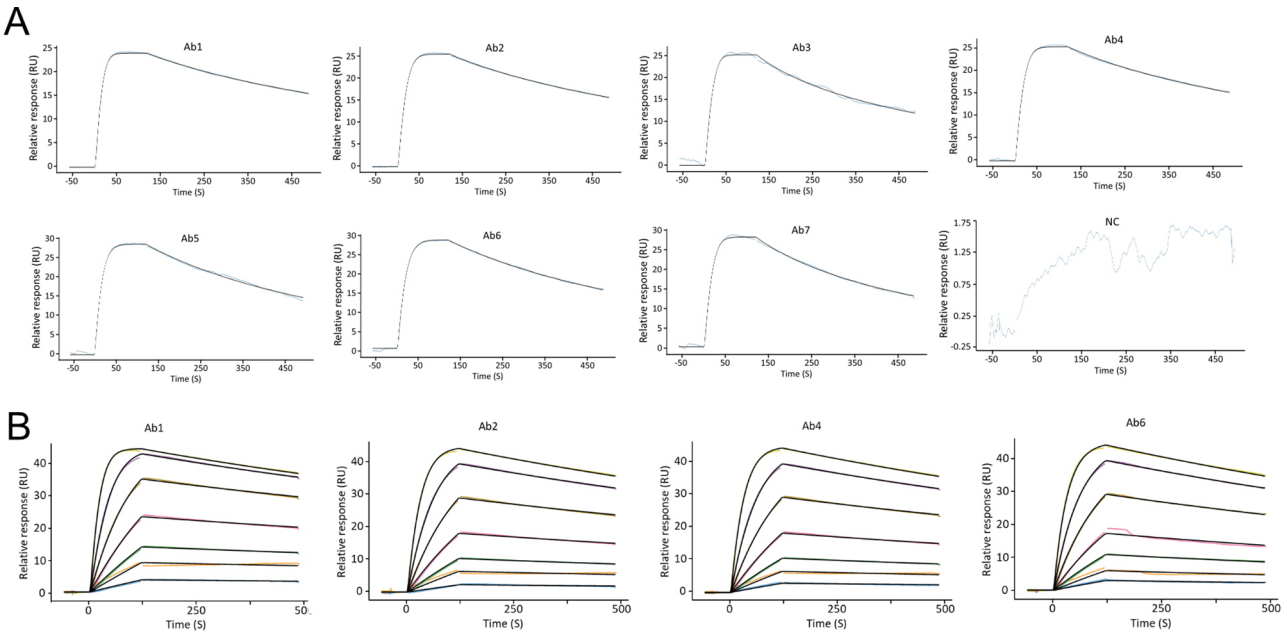

Fig. 2. Affinity ranking of humanized antibodies. (**A**) Sensor-grams showing affinity ranking of antibodies Ab1-Ab7 to biotin-conjugated antigen. The off-rates of antibodies were obtained from fitting the experimental data locally to 1:1 interaction model. Ab1: chimeric antibody. Ab2-7: humanized antibodies with back mutations to the FR region. NC: negative control. Sample concentration 400 nM. (**B**) Sensor-grams of the affinity measurement of biotin-conjugated antigen to antibodies Ab1, 2, 4, and 6. Sample concentration used are (in nM) 200, 100, 50, 25, 12.5, 6.25, 3.125. The colored lines represent the recorded binding response signals at different antigen concentrations, and the overlaid black lines represent the fitted curves.

Ligand	Analyte	Chi² (RU²)	ka (1/Ms)	kd (1/s)	KD (M)	Rmax (RU)
NC	peptide-biotin	NA	NA	NA	NA	NA
Ab1	peptide-biotin	1.61E-02	3.25E + 05	1.50E-03	4.61E-09	24.3
Ab2	peptide-biotin	2.24E-02	2.49E + 05	1.66E-03	6.66E-09	28.2
Ab3	peptide-biotin	2.66E-01	3.27E + 05	3.21E-03	9.81E-09	25.4
Ab4	peptide-biotin	4.42E-02	2.52E + 05	1.77E-03	7.00E-09	26.9
Ab5	peptide-biotin	8.68E-02	2.17E + 05	2.17E-03	9.96E-09	24
Ab6 (M4H)	peptide-biotin	5.72E-02	1.84E + 05	1.95E-03	1.06E-08	31.1
Ab7	peptide-biotin	9.44E-02	2.56E + 05	2.95E-03	1.15E-08	29.6

Table 1. Binding kinetics of antibody to antigen. NC: negative control; RU: response units; ka: association rate constant; kd: dissociation rate constant; KD: the equilibrium dissociation constants, kd = kd/ka; rmax: maximum analyte-ligand interaction response.

previous report indicating that TRPM4 blocking antibodies are species-specific[10]. It has been reported that ATP depletion after hypoxia activates TRPM4 channel[11] and TRPM4 blocking antibodies could directly inhibit TRPM4 currents[10,20–22]. Electrophysiology was thus employed to examine the functions of Ab1-7 in HEK 293 cells expressing human TRPM4. As TRPM4 can be activated by ATP depletion[11]an oxygen-glucose deprivation (OGD) buffer containing 5 mM NaN_3 and 10 mM 2-DG was applied to the HEK 293 cells expressing human TRPM4, in the control group treated with 20 μg/ml human IgG, 7-min ATP depletion significantly increased current (Fig. 1B, C). In all Ab1-7 treated cells, ATP depletion-induced current increase was successfully inhibited, suggesting that the humanized antibodies could directly inhibit human TRPM4 channels. It has been reported that HEK 293 cells express endogenous TRPM4 channel[23]. We recorded a small 8.8 pA current increase at + 80 mV holding potential following ATP depletion, which can be blocked by Ab6 (M4H) (Supplementary Fig. 1).

Binding affinity of humanized antibodies

To examine the binding affinity of antibodies to antigen, antibodies were captured on the sensor chip through the Fc capture method (Fig. 2A). The off-rates of antibodies were obtained from fitting the experimental data locally to 1:1 interaction model. The affinity of humanized Abs to antigen-biotin was summarized in Table 1. The dissociation rate constants (off-rates, kd) were calculated. Compared to chimeric antibody A1 (kd: 1.50E-03), the

binding affinity decreases in all humanized antibodies (kd: 1.66E-03 to 3.21E-03). Based on the ranking of kd, Ab2, Ab4, and Ab6 (M4H) were selected for further study. The affinity of antigen-biotin to purified antibodies Ab1, 2, 4, and Ab6 (M4H) was individually determined using a Surface Plasmon Resonance (SPR) biosensor, Biacore 8 K (Fig. 2B). The binding kinetics of antigen to antibodies were summarized in Table 2. The equilibrium dissociation constants (KD) were calculated from the ratio of kd over ka. The antigen binds to Ab2, 4 and Ab6 (M4H) in the order of Ab2 > Ab4 > Ab6 (M4H).

To examine the binding of humanized antibodies to TRPM4 channels on the surface of live cells, immunofluorescent staining was performed on live HEK 293 cells expressing myc-tagged human TRPM4. As shown in Fig. 3, application of Ab1, 2, 4, and Ab6 (M4H) to live HEK 293 cells had a strong surface staining co-localized with membrane marker Wheat Germ Agglutinin (WGA). Monoclonal antibody M4M exhibited a similar staining pattern. In contrast, control human IgG or polyclonal antibody M4P showed negative staining for human TRPM4. This result suggests that humanized antibodies are specific to human TRPM4 and can bind to TRPM4 channels on the cell membrane of live cells.

Stability of humanized antibodies Ab2, Ab4, and Ab6 (M4H)

The stability of an antibody can greatly influence its therapeutic performance[24]. We thus examined the stability of Ab2, 4, and Ab6 (M4H) under high temperature and low pH (Fig. 4). First, dynamic light scattering (DLS) was used to identify the temperature at which antibodies start to aggregate (Temperature onset/agg). Ab2, 4, and Ab6 (M4H) exhibited a DLS temperature of 64.21ºC, 62.11ºC, and 63.48ºC when aggregates were first detected at a radius of 6.8 nm, 8.96 nm, and 6.75 nm respectively (Fig. 4A). This result suggests that all 3 antibodies are stable until at least 62ºC. Next, capillary electrophoresis sodium dodecyl sulfate under non-reducing condition (CE-SDS-ND) was performed to study the antibodies stability under high temperature of 40 ºC for a duration up to 28 days. All 3 antibodies were stable for up to 14 days after incubation at 40 ºC. On day 28, the purity of Ab4 decreased, while the purity of Ab2 and Ab6 (M4H) remained stable (Fig. 4B). The main peak of Ab4 is 90.84%, lower than that for Ab2 (97.77%) and Ab6 (M4H) (97.76%), suggesting that around 10% Ab4 has degraded (Table 3). To test the antibody stability under acidic environment, the antibodies were incubated under a low pH of 3.5 for up to 4 h and examined using CE-SDS-ND (Fig. 4C). All 3 antibodies demonstrated excellent stability under pH 3.5 for 4 h. More than 99% antibodies were intact after pH 3.5 treatment (Table 4). As Ab4 is less stable than Ab2 and 6, we continued our study with Ab2 and 6.

Comparison of the inhibitory potency of Ab2, Ab6 (M4H) and M4M on ATP depletion-induced TRPM4 currents

It has been well established that ATP depletion under hypoxia conditions could activate TRPM4 channel. The TRPM4 blocking antibodies M4P and M4M have been shown to inhibit this ATP depletion-induced TRPM4 current increase[10,12,21,22]. To examine whether Ab2 and Ab6 (M4H) maintain the inhibitory function, M4M was first studied on HEK 293 cells transfected with human TRPM4 as a positive control. As shown in Fig. 5A, 7-min ATP depletion significantly induced TRPM4 current increase in control IgG treated cells. At doses of 10 and 20 μg/ml, M4M almost completely inhibited the current increase. The IC_{50} of M4M inhibition is 2.2 ± 1.8 μg/ml (Fig. 5B). For Ab2, doses of 5 and 10 μg/ml almost completely inhibited ATP depletion-induced current increase (Fig. 5C). The IC_{50} of Ab2 inhibition is 1.14 ± 1 μg/ml (Fig. 5D). For Ab6 (M4H), doses above 5 μg/ml completely inhibited ATP depletion-induced current increase (Fig. 5E). The IC_{50} of Ab6 (M4H) inhibition is 1.04 ± 1.3 μg/ml (Fig. 5F). There is no significance in IC_{50} among the three antibodies. As Ab6 (M4H) has the lowest IC_{50}, we proceeded to further study Ab6 (M4H) in human brain microvascular endothelial cells.

We further performed a structural modelling of Ab2, Ab4, and Ab6 (M4H) with TRPM4 channel as shown in Supplementary Fig. 2. Interestingly, Ab2 and Ab4 preferentially bind at the central tetrameric interface, whereas Ab6 (M4H) tends to bind at a peripheral site slightly offset from the center.

Preliminary characterization of Ab6 (M4H) in primary cultured human brain microvascular endothelial cells and animal model of stroke

For subsequent study, Ab6 is renamed M4H to represent its humanized source. In cultured human brain microvascular endothelial cells (HBMVECs), incubation of Ab6 (M4H) at a concentration of 10 μg/ml could downregulate baseline currents compared with control IgG (Fig. 6A, B). The increase in TRPM4 current induced by ATP depletion was then evaluated. Human brain microvascular endothelial cells (HBMVECs) were treated with either control human IgG or Ab6 (M4H). In the IgG treated HBMVECs, a 7-min ATP depletion significantly enhanced the TRPM4 current. (Fig. 6C, D). In contrast, Ab6 (M4H) treatment successfully suppressed the current increase following 7-min ATP depletion (Fig. 6E, F). Excessive Na^+ influx via TRPM4 is known to

Ligand	Analyte	Chi² (RU²)	ka (1/Ms)	kd (1/s)	KD (M)	Rmax (RU)
Ab1	peptide-biotin	1.24E-01	3.12E + 05	5.43E-04	1.74E-09	44.2
Ab2	peptide-biotin	1.04E-01	1.91E + 05	6.05E-04	3.16E-09	45.8
Ab4	peptide-biotin	7.35E-02	1.95E + 05	6.20E-04	3.18E-09	46.1
Ab6 (M4H)	peptide-biotin	1.62E-01	1.65E + 05	6.62E-04	4.02E-09	48.3

Table 2. Binding kinetics of antigen to antibodies. RU: response units; ka: association rate constant; kd: dissociation rate constant; KD: the equilibrium dissociation constants, kd = kd/ka; rmax: maximum analyte-ligand interaction response.

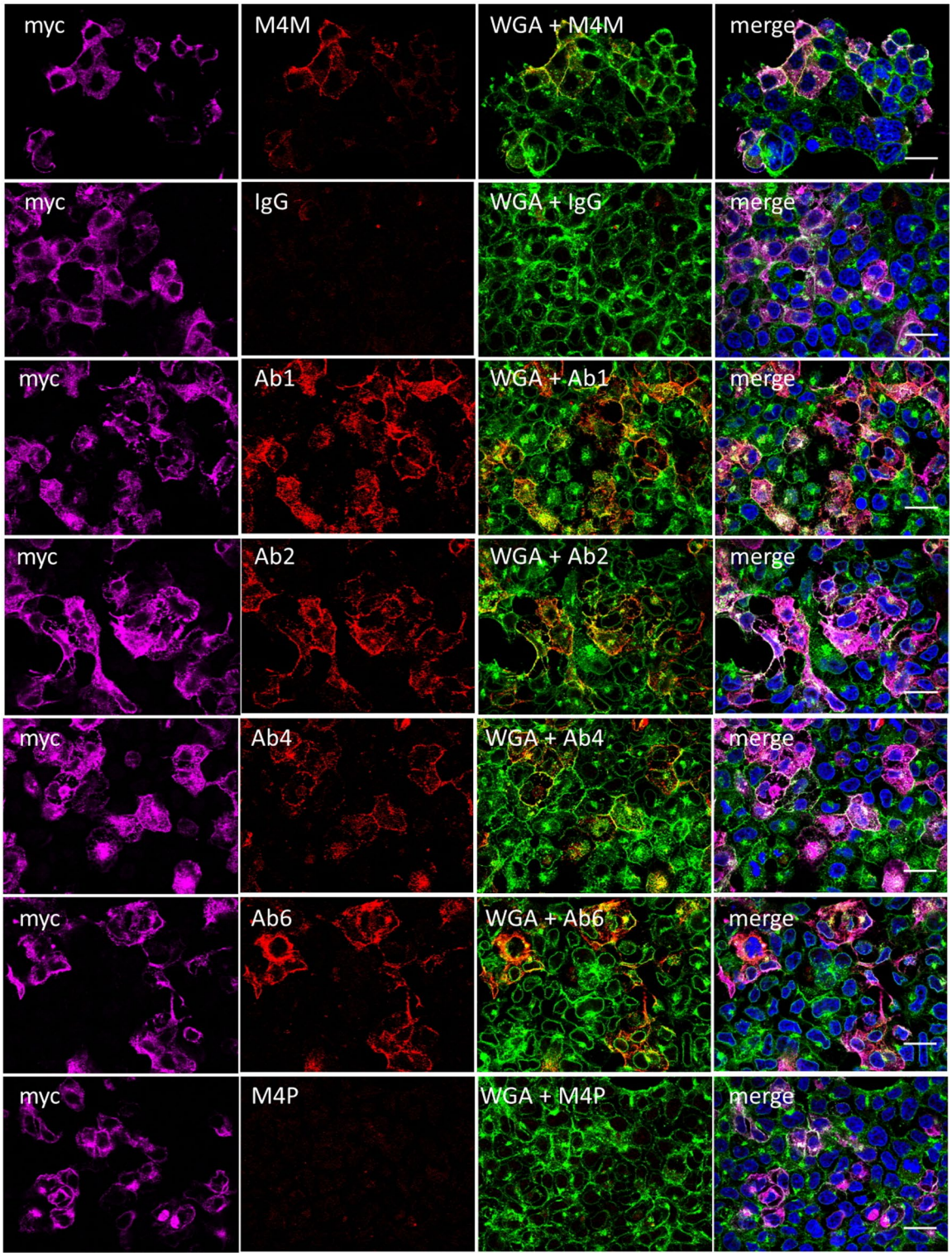

Fig. 3. Immunofluorescent staining of humanized antibodies on cells expressing human TRPM4. HEK 293 cells were transfected with myc-tagged human TRPM4 (labeled pink). Ab1, 2, 4, and Ab6 (M4H) (labeled red) were applied to live cells at 0.5 µg/ml for 1 h before fixation. Control IgG and M4P (labeled red) at 3 µg/ml are served as the negative control. M4M at 3 µg/ml is the positive control. The cell membrane was labeled green with Wheat Germ Agglutinin (WGA) and the nuclei were labeled with blue DAPI. Scale bars: 20 µm.

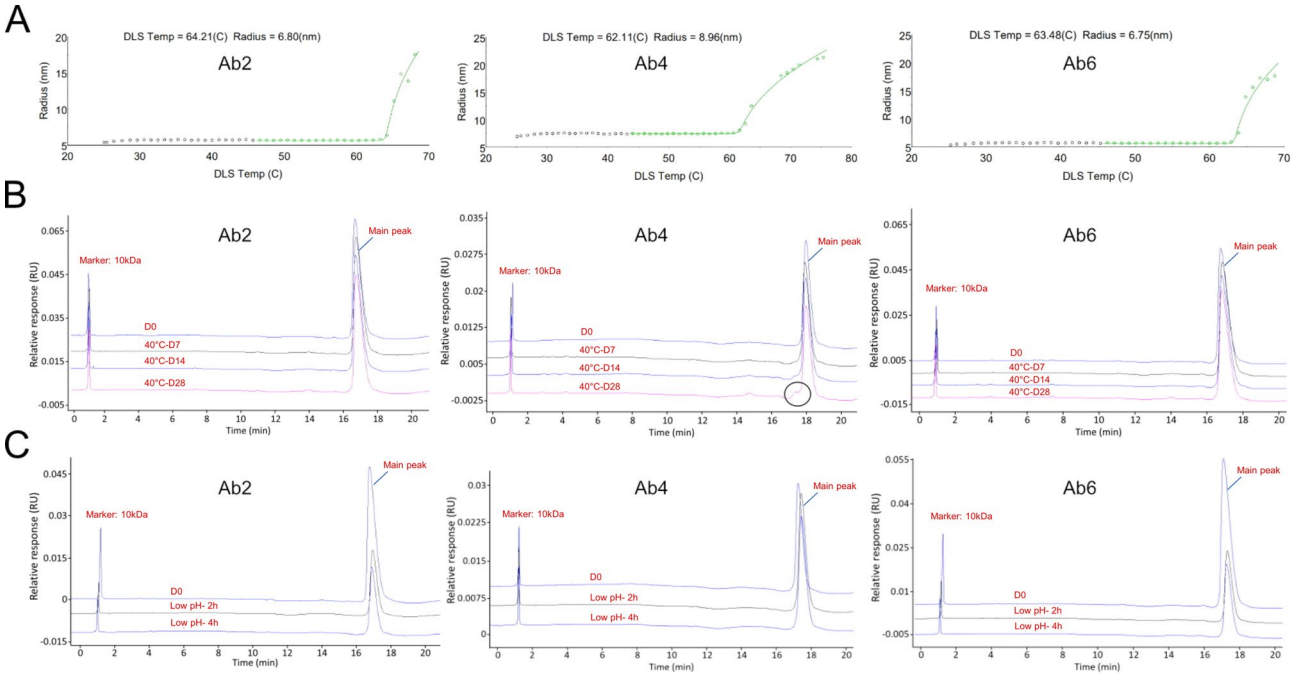

Fig. 4. Stability tests of Ab2, 4, and Ab6 (M4H) for higher temperature and low pH. (**A**) DLS (dynamic light scattering) thermogram of Ab2, 4, and 6. (**B**) CE-SDS-NR electropherograms of Ab2, 4, and Ab6 (M4H) of 40 °C stability taken at D0 (day 0), D7 (day 7), D14 (day 14) and D28 (day). D0 indicates the starting point. For Ab4 at 40 °C, 28 days showed some decreased purity of CE-SDS (encircled). (**C**) CE-SDS-NR electropherograms of Ab2, 4, and Ab6 (M4H) of low pH3.5 stability for 0 (D0), 2 and 4 h.

Sample name	Conditions / Time points	UV280 Conc. (mg/mL)	CE-SDS-NR Main (%)
Ab2	D0	2.61	99.37
	40ºC -D7	2.52	98.28
	40 ºC -D14	2.67	98.49
	40 ºC -D28	2.57	97.77
Ab4	D0	2.68	99.90
	40 ºC -D7	2.70	98.87
	40 ºC -D14	2.68	96.18
	40 ºC -D28	2.76	90.84
Ab6 (M4H)	D0	3.03	99.28
	40 ºC -D7	2.96	98.75
	40 ºC -D14	2.97	98.42
	40 ºC -D28	2.90	97.76

Table 3. 40℃ stability test results. CE-SDS-NR: non-reducing capillary electrophoresis sodium Dodecyl sulfate.

increase cell volume[22], we then observed the morphological changes in HBMVECs under 7-min ATP depletion (Fig. 6G). Under control human IgG treatment, the cell area was increased after ATP depletion, whereas in cells under Ab6 (M4H) treatment, the morphology remains relatively unchanged. We further calculated the change of cell membrane capacitance (C_m) which is an indicator of cell volume[10]. In control human IgG treated HBMVECs, the C_m started to increase 1 min after OGD buffer treatment (Fig. 6H). After 10 min, the C_m was increased by around 30%. In Ab6 (M4H) treated HBMVECs, the C_m was increased slowly by around 5% at 4 min. The C_m was kept relatively stable after that. After 2 min, the C_m of IgG treated cells was significantly higher than that of the Ab6 (M4H) treated cells. It should be noted that Ab6 (M4H) has no effect on TRPM4 close family members TRPM2, 5 and 7 (Supplementary Fig. 3).

Using WGA as a cell membrane marker[10]we found that Ab6 (M4H) binds to the cell membrane of live HBMVECs under hypoxia, but not HBMVECs under normoxia (Supplementary Fig. 4). The specificity of Ab6 (M4H) was further verified using a transgenic rat model carrying human TRPM4 sequence[19]. Middle cerebral

Sample name	Conditions / Time points	UV280	CE-SDS-NR
		Conc. (mg/mL)	Main (%)
Ab2	D0	2.61	99.37
	Low pH-2 h	3.09	99.89
	Low pH-4 h	3.06	99.83
Ab4	D0	2.68	99.90
	Low pH-2 h	3.23	99.87
	Low pH-4 h	3.38	99.85
Ab6 (M4H)	D0	3.03	99.28
	Low pH-2 h	3.18	99.88
	Low pH-4 h	3.28	99.91

Table 4. Low pH 3.5 stability test results. CE-SDS-NR: non-reducing capillary electrophoresis sodium Dodecyl sulfate.

artery occlusion (MCAO) was created in the rats to induce stroke. In wild type MCAO rats, Ab6 (M4H) was negatively stained in both ipsilateral and contralateral hemispheres (Supplementary Fig. 5A). In transgenic rats carrying human TRPM4, Ab6 (M4H) was strongly co-stained with endothelial marker vWF in the ipsilateral hemisphere, but not in the contralateral hemisphere (Supplementary Fig. 5B). This result is consistent with our previous studies showing that TRPM4 is upregulated in vascular endothelial cells in the ipsilateral hemisphere of stroke animals[25,26].

Discussion

TRPM4 channel is an ideal drug target due to its low expression in the brain and unique electrophysiological properties[6,10,27,28]. TRPM4 inhibition by antisense oligodeoxynucleotide or siRNA has been shown to protect vasculature in spinal cord injury[11] and stroke models of both permanent and transient middle cerebral artery occlusion[25,26]. In the animal model of chronic global cerebral hypoxia, treatment with TRPM4 siRNA rescued LTP impairment and prevented the reduction of synaptic proteins such as brain-derived neurotrophic factor (BDNF)[29]. However, a major drawback of silencing TRPM4 expression is that, when used to treat acute diseases, they must be administered at an early stage of disease onset before protein upregulation. In addition, siRNA does not directly block the channel. Therefore, we decided to develop a channel-specific antibody that can directly block TRPM4.

The polyclonal antibody M4P was first produced against the rat TRPM4 channel[21]. By targeting an extracellular motif close to the channel pore, M4P was shown to block TRPM4 current and downregulate surface expression upon sustained incubation. After ATP depletion, M4P successfully inhibited the cell swelling of neurons and vascular endothelial cells, but not astrocytes[22]. Excitingly, treatment of M4P could prevent membrane depolarization after chronic hypoxia, thereby ameliorating glutamate-induced excitotoxicity by maintaining magnesium blockade of NMDA receptors[12]. In addition to direct channel blocking effect, TRPM4 antibodies have the following advantages over existing blockers. The antibodies are highly specific to TRPM4 channel[20]. After prolonged binding, TRPM4 antibodies could downregulate surface TRPM4 channels for internalization[10,21]. Additionally, therapeutic antibodies have a longer plasma half-life than small molecules[30–33]. Therefore, TRPM4 blocking antibody is superior to small molecules that simply block the channel. In vivo studies on animal models of stroke revealed that M4P could attenuate reperfusion injury in both early[21] and delayed[18] recanalization, potentially extending the reperfusion time window.

As M4P does not cross-react with human TRPM4, a mouse monoclonal antibody M4M was developed by targeting a similar extracellular motif[10]. M4M retains the properties of M4P, such as inhibition of human TRPM4 currents and downregulation of surface expression of human TRPM4. The epitope recognized by M4M has been identified as a four-amino acid sequence EPGF that is close to the channel pore[20]. Substitution of either amino acid completely abolished M4M binding, explaining why M4M and M4P are species-specific, as the corresponding sequences in mouse and rat are ERGS. To characterize M4M, we generated a transgenic rat carrying human TRPM4 sequence. When stroke model was established in the transgenic rats, M4M was shown to reduce reperfusion injury[19]suggesting that M4M is specific for human TRPM4.

Antibody humanization is a key step in reducing the immunogenicity of xenogeneic-derived antibodies, it allows mouse monoclonal antibodies to be used in humans[34,35]. We performed M4M humanization in this study as a key step towards therapy. Human IgG1 was introduced into M4M using the CDR grafting method to replace mouse IgG[36]. By retaining the antigen-binding CDR regions while replacing non-human sequences with human counterparts, this technique helps minimize immunogenic side effects. As antibody humanization could reduce binding affinity[37]various back mutations were introduced to enhance binding affinity. However, all humanized antibodies demonstrated some degree of reduction on binding affinity (Table 1). Meanwhile, they all completely inhibited TRPM4 current induced by ATP depletion at a concentration of 20 μg/ml and showed no cross-reactivity with rodent TRPM4. Furthermore, Ab6 (M4H) does not bind to human TRPM4 channel close members human TRPM2, 5, and 7. The top 3 clones are relatively stable under high temperatures and low pH, with Ab2 and Ab6 (M4H) outperforming Ab4. Surface labelling indicated that the humanized antibodies could bind to human TRPM4 channels on the cell membrane of live cells, suggesting that these antibodies can access

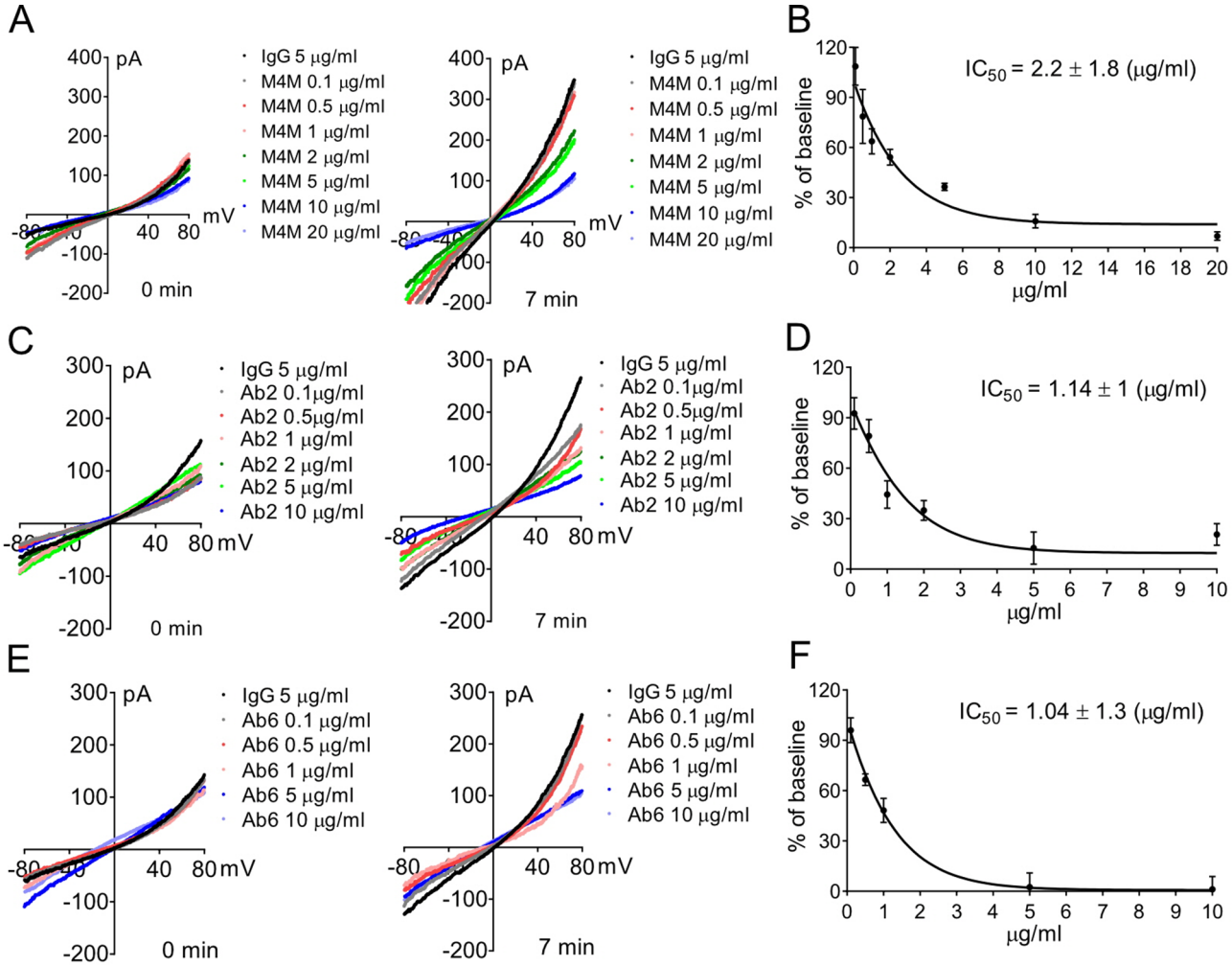

Fig. 5. Dose-dependent inhibition of human TRPM4 by Ab2 and Ab6 (M4H). (**A**) Current-voltage relationship of HEK 293 cells expressing human TRPM4 that were incubated with 5 μg/ml control IgG or M4M at concentrations of 0.1–20 μg/ml for 30 min before ATP depletion was induced. Voltage ramps from − 80 to 80 mV were applied at 0 min and 7 min. $N = 7, 6, 6, 6, 6, 6, 6, 6$ for IgG and different concentrations of M4M. (**B**) Dose-response curve (from A) shows that M4M inhibits the ATP depletion-induced increase in human TRPM4 currents in a dose-dependent manner. Values are normalized to IgG. IC_{50} was calculated from fit of dose–response curve to the Hill equation. (**C**) Current-voltage relationship of human TRPM4 before and after 7-min ATP depletion. The cells were treated with control IgG (5 μg/ml) or Ab2 at doses of 0.1–10 μg/ml for 30 min before ATP depletion in HEK 293 cells. $N = 7, 6, 6, 5, 7, 6, 6$ for IgG and different concentrations of Ab2. (**D**) The dose-response curve (from C) of Ab2 treatment. Values are normalized to IgG. IC_{50} was calculated from fit of dose–response curve to the Hill equation. (**E**) Current-voltage relationship of human TRPM4 with treatment of control IgG or Ab6 (M4H) at concentrations of 0.1–10 μg/ml for 30 min before ATP depletion in HEK 293 cells. $N = 7, 7, 6, 5, 7, 8$ for IgG (5 μg/ml) and different concentrations of Ab6 (M4H). (**F**) The dose-response curve (from E) of Ab6 (M4H) treatment. Values are normalized to IgG, IC_{50} was calculated from fit of dose–response curve to the Hill equation.

the channels from extracellular space and yield the inhibitory effect. This result is consistent with our previous studies on M4P and M4M[10,21].

Interestingly, although antibody-antigen affinity studies showed that the humanization process reduced binding affinity, electrophysiological studies revealed that the IC_{50}s of Ab2 and Ab6 (M4H) were no lower than that of M4M, or maybe even better. This is possibly due to the different experimental conditions as the antibody-antigen affinity studies were performed at peptide level, whereas electrophysiological studies were carried out on full channels on live cells. It is better to use full-length channel for binding assay. However, as TRPM4 channel contains 6 transmembrane segments, it remains a challenge to obtain full-length channel with proper folding. Studies using Ab6 (M4H) on HBMVECs showed that the humanized antibody effectively inhibited ATP depletion-induced cell swelling by inhibiting TRPM4 currents. Thus, TRPM4 humanized antibodies can yield a protective function on native human cells and shows promise for therapeutic applications. The actual therapeutic dose shall be optimized in animal models.

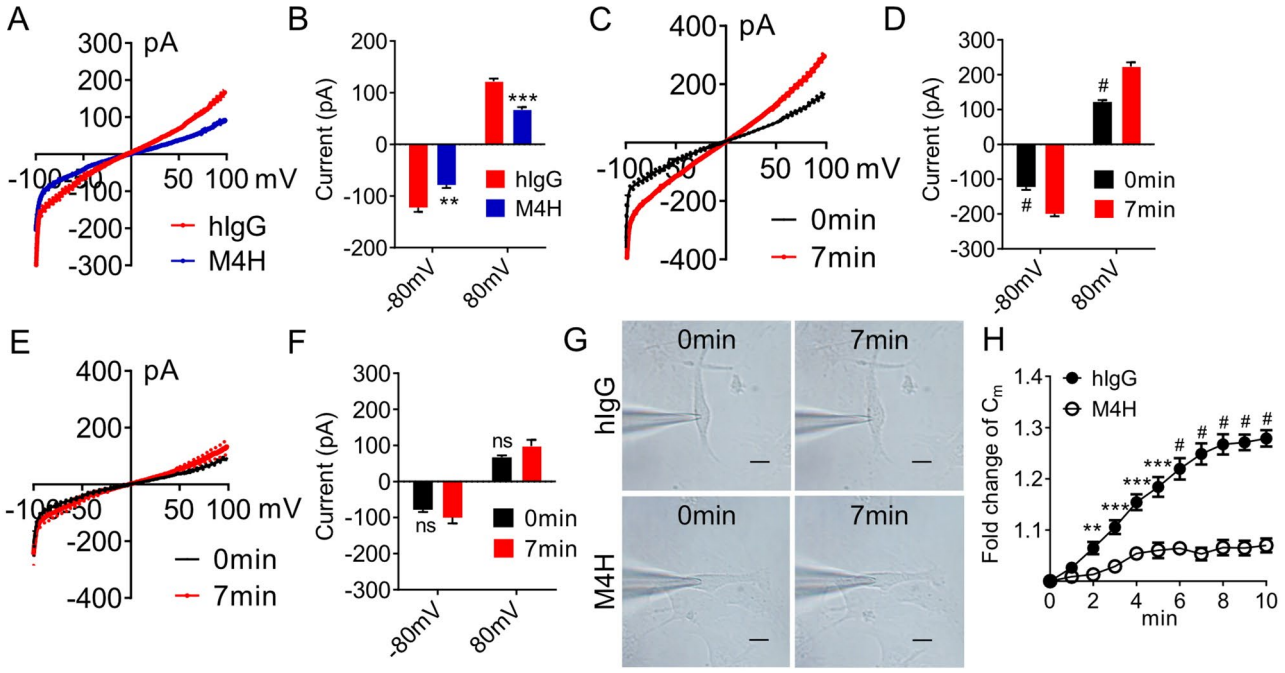

Fig. 6. Effect of Ab6 (M4H) on cultured human microvascular endothelial cells (HMVECs). (**A**) Current-voltage relationship of HMVECs that were cultured with control human IgG or Ab6 (M4H) (10 µg/ml) for 30 min before voltage ramps from – 100 to 100 mV were applied. $N=7$ cells for both groups. (**B**) Summary of currents at – 80 or 80 mV from A. (**C**) Current-voltage relationship of HMVECs that were first cultured with control human IgG (10 µg/ml) for 30 min. Followed by ATP depletion by solution containing 5 mM NaN_3 and 10 mM 2-DG applied around 10 µm away from the recording cells. Voltage ramps from – 100 to 100 mV were applied at baseline 0 min and 7 min after ATP depletion treatment. $N=7$ cells for both groups. (**D**) Summary of currents at – 80 or 80 mV from C. (**E**) Voltage ramps from – 100 to 100 mV at baseline 0 min and 7 min after ATP depletion were applied in cells treated with Ab6 (M4H) (10 µg/ml). $N=7$ cells for both groups. (**F**) Summary of currents at – 80 or 80 mV from E. (**G**) Sample images of HMVECs treated with control human IgG or Ab6 (M4H) (10 µg/ml) before and after 7-min ATP depletion. Scale bars: 10 µm. (**H**) Comparison of membrane capacitance (C_m) changes for HMVECs treated with control human IgG and Ab6 (M4H) under ATP depletion induced by 5-mM NaN_3 and 10-mM 2-DG for 10 min. In (**B**, **D**, **F**), statistical analysis was performed by Student's *t* test and in H by two-way ANOVA with the Bonferroni post hoc test. $^{**}P<0.01$, $^{***}P<0.001$, $^{\#}P<0.0001$.

In conclusion, we have successfully humanized the anti-TRPM4 antibodies for potential use in humans. These humanized antibodies retain the properties of previously studied polyclonal and mouse monoclonal antibodies. The next stage would be to ensure the efficacy of the humanized antibody by in vivo studies using animal models of diseases. Previous in vivo studies on M4M were carried out in rats[19]. Being a mouse monoclonal antibody, M4M is less likely to produce adverse side effects in rodents. Although we have generated a humanized rat model to carrying human TRPM4 sequence, the immune system remains to be of rodent origin. Potential immunogenicity may arise when the humanized antibodies are introduced into the rodents, particularly under repeated injections[38,39]. If the humanized antibodies are used in managing acute diseases with a single dose injection such as in stroke, the effect of immunogenicity can be greatly reduced. Furthermore, humanized antibodies may have different pharmacokinetic and pharmacodynamic properties in rodents, which may affect therapeutic efficacy in preclinical studies[40–42].

Data availability

All data reported in this paper are available from the corresponding author, P.L., upon reasonable request.

Received: 11 December 2024; Accepted: 2 June 2025
Published online: 05 June 2025

References

1. Mathar, I. et al. Trpm4. *Handb. Exp. Pharmacol.* **222**, 461–487. https://doi.org/10.1007/978-3-642-54215-2_18 (2014).
2. Gao, Y. & Liao, P. TRPM4 channel and cancer. *Cancer Lett.* **454**, 66–69. https://doi.org/10.1016/j.canlet.2019.04.012 (2019).
3. Hu, J. et al. Physiological temperature drives TRPM4 ligand recognition and gating. *Nature* **630**, 509–515. https://doi.org/10.1038/s41586-024-07436-7 (2024).
4. Guinamard, R., Demion, M. & Launay, P. Physiological roles of the TRPM4 channel extracted from background currents. *Physiol. (Bethesda)*. **25**, 155–164. https://doi.org/10.1152/physiol.00004.2010 (2010).

5. Dienes, C. et al. Pharmacological modulation and (Patho)Physiological roles of TRPM4 Channel-Part 2: TRPM4 in health and disease. *Pharmaceuticals* **15** https://doi.org/10.3390/ph15010040 (2021).
6. Zhang, E. & Liao, P. Brain transient receptor potential channels and stroke. *J. Neurosci. Res.* **93**, 1165–1183. https://doi.org/10.1002/jnr.23529 (2015).
7. Pringle, A. K. In, out, shake it all about: elevation of [Ca2+]i during acute cerebral ischaemia. *Cell. Calcium.* **36**, 235–245. https://doi.org/10.1016/j.ceca.2004.02.014 (2004).
8. Kristian, T. & Siesjo, B. K. Calcium in ischemic cell death. *Stroke* **29**, 705–718. https://doi.org/10.1161/01.str.29.3.705 (1998).
9. Schattling, B. et al. TRPM4 cation channel mediates axonal and neuronal degeneration in experimental autoimmune encephalomyelitis and multiple sclerosis. *Nat. Med.* **18**, 1805–1811. https://doi.org/10.1038/nm.3015 (2012).
10. Low, S. W. et al. Development and characterization of a monoclonal antibody blocking human TRPM4 channel. *Sci. Rep.* **11**, 10411. https://doi.org/10.1038/s41598-021-89935-5 (2021).
11. Gerzanich, V. et al. De Novo expression of Trpm4 initiates secondary hemorrhage in spinal cord injury. *Nat. Med.* **15**, 185–191. https://doi.org/10.1038/nm.1899 (2009).
12. Poore, C. P. et al. TRPM4 blocking antibody reduces neuronal excitotoxicity by specifically inhibiting glutamate-induced calcium influx under chronic hypoxia. *Neurobiol. Dis.* **191**, 106408. https://doi.org/10.1016/j.nbd.2024.106408 (2024).
13. Rajamanickam, G., Hu, Z. & Liao, P. Targeting the TRPM4 channel for neurologic diseases: opportunity and challenge. *Neuroscientist: Rev. J. Bringing Neurobiol. Neurol. Psychiatry.* **10738584251318979** https://doi.org/10.1177/10738584251318979 (2025).
14. Burris, S. K., Wang, Q., Bulley, S., Neeb, Z. P. & Jaggar, J. H. 9-Phenanthrol inhibits Recombinant and arterial myocyte TMEM16A channels. *Br. J. Pharmacol.* **172**, 2459–2468. https://doi.org/10.1111/bph.13077 (2015).
15. Bostrom, C. E. et al. Cancer risk assessment, indicators, and guidelines for polycyclic aromatic hydrocarbons in the ambient air. *Environ. Health Perspect.* **110** (Suppl 3), 451–488 (2002).
16. Kurland, D. B. et al. Glibenclamide for the treatment of acute CNS injury. *Pharmaceuticals* **6**, 1287–1303 (2013). [pii]10.3390/ph6101287.
17. Groop, L. et al. Comparison of pharmacokinetics, metabolic effects and mechanisms of action of glyburide and glipizide during long-term treatment. *Diabetes Care.* **10**, 671–678. https://doi.org/10.2337/diacare.10.6.671 (1987).
18. Chen, B. et al. TRPM4 blocking antibody protects cerebral vasculature in delayed stroke reperfusion. *Biomedicines* **11** https://doi.org/10.3390/biomedicines11051480 (2023).
19. Poore, C. P. et al. In vivo evaluation of monoclonal antibody M4M using a humanised rat model of stroke demonstrates Attenuation of reperfusion injury via blocking human TRPM4 channel. *J. Drug Target.* **32**, 413–422. https://doi.org/10.1080/1061186X.2024.2313522 (2024).
20. Wei, S. et al. Binding epitope for recognition of human TRPM4 channel by monoclonal antibody M4M. *Sci. Rep.* **12**, 19562. https://doi.org/10.1038/s41598-022-22077-4 (2022).
21. Chen, B. et al. TRPM4-specific blocking antibody attenuates reperfusion injury in a rat model of stroke. *Pflugers Arch.* **471**, 1455–1466. https://doi.org/10.1007/s00424-019-02326-8 (2019).
22. Wei, S. et al. Comparison of Anti-oncotic effect of TRPM4 blocking antibody in neuron, astrocyte and vascular endothelial cell under hypoxia. *Front. Cell. Dev. Biol.* **8**, 562584. https://doi.org/10.3389/fcell.2020.562584 (2020).
23. Amarouch, M. Y., Syam, N. & Abriel, H. Biochemical, single-channel, whole-cell patch clamp, and Pharmacological analyses of endogenous TRPM4 channels in HEK293 cells. *Neurosci. Lett.* **541**, 105–110. https://doi.org/10.1016/j.neulet.2013.02.011 (2013).
24. Ma, H., O'Fagain, C. & O'Kennedy, R. Antibody stability: A key to performance - Analysis, influences and improvement. *Biochimie* **177**, 213–225. https://doi.org/10.1016/j.biochi.2020.08.019 (2020).
25. Loh, K. P. et al. TRPM4 Inhibition promotes angiogenesis after ischemic stroke. *Pflugers Arch.* **466**, 563–576. https://doi.org/10.1007/s00424-013-1347-4 (2014).
26. Chen, B. et al. Non-Invasive multimodality imaging directly shows TRPM4 Inhibition ameliorates stroke reperfusion injury. *Transl Stroke Res.* **10**, 91–103. https://doi.org/10.1007/s12975-018-0621-3 (2019).
27. Borgstrom, A., Peinelt, C. & Stoklosa, P. TRPM4 in Cancer-A new potential drug target. *Biomolecules* **11** https://doi.org/10.3390/biom11020229 (2021).
28. Borgstrom, A. et al. Small molecular inhibitors block TRPM4 currents in prostate Cancer cells, with limited impact on Cancer hallmark functions. *J. Mol. Biol.* **433**, 166665. https://doi.org/10.1016/j.jmb.2020.09.024 (2021).
29. Hazalin, N., Liao, P. & Hassan, Z. TRPM4 Inhibition improves Spatial memory impairment and hippocampal long-term potentiation deficit in chronic cerebral hypoperfused rats. *Behav. Brain Res.* **393**, 112781. https://doi.org/10.1016/j.bbr.2020.112781 (2020).
30. Foss, S. et al. Human IgG Fc-engineering for enhanced plasma half-life, mucosal distribution and killing of cancer cells and bacteria. *Nat. Commun.* **15**, 2007. https://doi.org/10.1038/s41467-024-46321-9 (2024).
31. Lu, R. M. et al. Development of therapeutic antibodies for the treatment of diseases. *J. Biomed. Sci.* **27**, 1. https://doi.org/10.1186/s12929-019-0592-z (2020).
32. Haraya, K., Tachibana, T. & Igawa, T. Improvement of Pharmacokinetic properties of therapeutic antibodies by antibody engineering. *Drug Metab. Pharmacokinet.* **34**, 25–41. https://doi.org/10.1016/j.dmpk.2018.10.003 (2019).
33. Toledo-Stuardo, K. et al. Therapeutic antibodies in oncology: an Immunopharmacological overview. *Cancer Immunol. Immunotherapy: CII.* **73**, 242. https://doi.org/10.1007/s00262-024-03814-2 (2024).
34. Almagro, J. C. & Fransson, J. Humanization of antibodies. *Front. Bioscience: J. Virtual Libr.* **13**, 1619–1633. https://doi.org/10.2741/2786 (2008).
35. Clavero-Alvarez, A., Di Mambro, T., Perez-Gaviro, S., Magnani, M. & Bruscolini, P. Humanization of antibodies using a statistical inference approach. *Sci. Rep.* **8**, 14820. https://doi.org/10.1038/s41598-018-32986-y (2018).
36. Lo, B. K. Antibody humanization by CDR grafting. *Methods Mol. Biol.* **248**, 135–159. https://doi.org/10.1385/1-59259-666-5 (2004).
37. Baca, M., Presta, L. G., O'Connor, S. J. & Wells, J. A. Antibody humanization using monovalent phage display. *J. Biol. Chem.* **272**, 10678–10684. https://doi.org/10.1074/jbc.272.16.10678 (1997).
38. Harding, F. A., Stickler, M. M., Razo, J. & DuBridge, R. B. The immunogenicity of humanized and fully human antibodies: residual immunogenicity resides in the CDR regions. *MAbs* **2**, 256–265. https://doi.org/10.4161/mabs.2.3.11641 (2010).
39. Lee, E. C. et al. Complete humanization of the mouse Immunoglobulin loci enables efficient therapeutic antibody discovery. *Nat. Biotechnol.* **32**, 356–363. https://doi.org/10.1038/nbt.2825 (2014).
40. Betts, A. et al. Linear Pharmacokinetic parameters for monoclonal antibodies are similar within a species and across different Pharmacological targets: A comparison between human, cynomolgus monkey and hFcRn Tg32 Transgenic mouse using a population-modeling approach. *mAbs* **10**, 751–764. https://doi.org/10.1080/19420862.2018.1462429 (2018).
41. Kamath, A. V. Translational pharmacokinetics and pharmacodynamics of monoclonal antibodies. *Drug Discovery Today Technol.* **21–22**, 75–83. https://doi.org/10.1016/j.ddtec.2016.09.004 (2016).
42. Dostalek, M., Gardner, I., Gurbaxani, B. M., Rose, R. H. & Chetty, M. Pharmacokinetics, pharmacodynamics and physiologically-based Pharmacokinetic modelling of monoclonal antibodies. *Clin. Pharmacokinet.* **52**, 83–124. https://doi.org/10.1007/s40262-012-0027-4 (2013).

Acknowledgements
This work was supported by grants: MOH-001361-00 and MOH-001384-00 from the Singapore Ministry of Health's National Medical Research Council.

Author contributions
P.L. and H.F conceived and directed the project; S.W., C.P.P, H.F., and P.L. conceived, analyzed data, and wrote the paper; S.W., C.P.P., R.K.V, S.W.L., B.C. performed experiments and analyzed data. All authors reviewed the manuscript.

Declarations

Competing interests
The authors declare no competing interests.

Additional information
Supplementary Information The online version contains supplementary material available at https://doi.org/10.1038/s41598-025-05256-x.

Correspondence and requests for materials should be addressed to H.F. or P.L.

Reprints and permissions information is available at www.nature.com/reprints.

Publisher's note Springer Nature remains neutral with regard to jurisdictional claims in published maps and institutional affiliations.